Ramon G. Rubio • Yuri S. Ryazantsev
Victor M. Starov • Guo-Xiang Huang
Alexander P. Chetverikov • Paolo Arena
Alex A. Nepomnyashchy • Alberto Ferrus
Eugene G. Morozov
Editors

Without Bounds: A Scientific Canvas of Nonlinearity and Complex Dynamics

Springer

Editors
Ramon G. Rubio
Dpt. Quimica-Fisica-I
UCM
Madrid, Spain

Yuri S. Ryazantsev
Instituto Pluridisciplinar
UCM
Madrid, Spain

Victor M. Starov
Dpt. of Chemical Engineering
Loughborough University
Loughborough, United Kingdom

Guo-Xiang Huang
Physics Dpt.
East China Normal University
Shanghai
China, People's Republic

Alexander P. Chetverikov
Faculty of Physics
Saratov State University
Saratov, Russia

Paolo Arena
Dpt. di Ingegneria Elettrica
Elettronica
Università di Catania
Catania, Italy

Alex A. Nepomnyashchy
Dept. of Mathematics
Technion
Haifa, Israel

Alberto Ferrus
Instituto Cajal
CSIC
Madrid, Spain

Eugene G. Morozov
Shirshov Institute of Oceanology
Moscow, Russia

ISSN 1860-0832 ISSN 1860-0840 (electronic)
ISBN 978-3-642-34069-7 ISBN 978-3-642-34070-3 (eBook)
DOI 10.1007/978-3-642-34070-3
Springer Heidelberg New York Dordrecht London

Library of Congress Control Number: 2013937955

Cohesive and Non-cohesive Adsorption of Surfactants at Liquid Interfaces

R.I. Slavchov, I.M. Dimitrova, and I.B. Ivanov

1 Introduction

Long ago, Adam showed that the spread monolayers of nonionic surfactants exhibit a state with the properties of a two-dimensional (2D) liquid [1], e.g., with compressibility intermediate between that of the 2D gaseous and the 2D solid states of the adsorption layers. Consequently, he called this 2D phase "liquid expanded (LE)" [1–3]. The reasons for its existence and its basic structure were revealed by Langmuir [2]. He argued that the hydrocarbon tails of the surfactant in the LE state form a very thin liquid oil film spread over the interface.

The concept of LE monolayer is not widely accepted for the most important from technological point of view soluble adsorption layers at liquid interfaces. The most popular adsorption isotherms used in the literature for soluble surfactants (Volmer, de Boer-van der Waals, Langmuir's isotherm for soluble surfactants, Frumkin) do not involve the LE state and the phase transition from 2D gas to LE. The reason of the neglect of such phase transition is the fact that it is not easy to observe it with surface tension data: it occurs as a small kink (discontinuity of the first derivative) in the dependence of the surface tension σ on the concentration C which is often obscured by the experimental error. Several studies exist which give evidence that LE state is, in fact, common feature not only of insoluble, but also to soluble monolayers [4–7]. Still, to the best of our knowledge, answers have not been given to the following basic questions: which soluble surfactants exhibit the LE state and which ones do not? How to prove the existence of LE state and when to expect it? How are the parameters of the LE state related to the surfactant structure and the

R.I. Slavchov · I.M. Dimitrova
Department of Physical Chemistry, Sofia University, 1164 Sofia, Bulgaria

I.B. Ivanov (✉)
Laboratory of Chemical Physics and Engineering, Sofia University, 1164 Sofia, Bulgaria
e-mail: ii@lcpe.uni-sofia.bg

R.G. Rubio et al. (eds.), *Without Bounds: A Scientific Canvas of Nonlinearity and Complex Dynamics*, Understanding Complex Systems,
DOI 10.1007/978-3-642-34070-3_22,

medium properties (temperature, composition, etc.)? A previous work of ours dealt with the LE state in monolayers of ionic surfactants [6]. In this work, we turn to uncharged adsorption layers of soluble nonionic surfactants.

Two types of surface pressure isotherms (surface pressure $\pi^S \equiv \sigma_0 - \sigma$ vs. concentration C) will be considered in this chapter: cohesive and non-cohesive. The non-cohesive type of isotherms start at $\pi^S = 0$ and $C = 0$ with a linear portion. At larger concentrations, the dependence π^S vs. C smoothly becomes curved, with negative deviations from the ideal behavior, corresponding to repulsion (cf. Figs. 2a and 3 below).

In the case of cohesive type of isotherm, the initial linear portion starts again at $\pi^S = 0$ and $C = 0$. Then, at relatively low concentrations, $\pi^S(C)$ undergoes a kink, followed by a second linear portion of larger slope and negative intercept $-\pi_{coh}$ (cf. Fig. 2a). The first linear portion corresponds to 2D gaseous layer, where Henry's adsorption isotherm holds. The second linear portion corresponds to LE layer. With *insoluble* surfactants, the LE layer at larger compressions undergoes phase transition to a solid like layer [1–3,8]. With *soluble* surfactants, the adsorption isotherm eventually curves due to repulsion between the hydrophilic heads and π^S stops changing when the critical micelle concentration (*cmc*) is reached. These events will be discussed in details in Sect. 3.

Langmuir's suggestion for the structure of the LE layer was that, in fact, an oil-like film is formed by the surfactant hydrophobic tails at which the hydrophilic groups are "adsorbed" [2]. He argued that this layer "must be regarded as essentially a typical hydrocarbon liquid in which the molecules possess all natural freedom of motion of such liquids" [2]. Kaganer et al. also pointed out that the LE layer is structureless and "there is no detectable X-ray diffraction signal. In this phase, the heads of the molecules are translationally disordered and the chains are conformationally disordered" [8]. Langmuir showed that his model explains the main feature of the 2D equation of state (EOS): the existence of what he called "spreading pressure of the monolayer" (we prefer the notion cohesive pressure, π_{coh}, introduced later by Davies [9, 10]). Later, Langmuir's model was extended several times. For example, the repulsion between the surfactant polar head-groups was treated by Smith [11], and the dependence of the cohesive pressure on the adsorption was analyzed by Davies [9, 10]. In *soluble* monolayers, first order phase transitions of the LE phase both to 2D-gaseous and to 2D-solid state were directly observed by Brewster angle microscopy and dynamic surface tension measurements [5]. For the current state of the art of the phase behavior of *insoluble* monolayers, the reader is referred to the available reviews in the literature [8, 12].

Langmuir analyzed further the equation of state (π^S vs. surface area A) of films of myristic acid spread on a dilute HCl solution around the point of phase transition to the solid-like layer. He argued that the data for this region can be explained if one assumes that surface aggregates (micelles) of 13 molecules are in equilibrium at the surface with single molecules [2]. Kumpulainen et al. [4] applied this idea to explain their tensiometric data obtained for soluble surfactants. Large surface aggregates were detected experimentally by optical methods, e.g., fluorescence micrography [13].

In this paper we are interested mainly in the linear part of the LE adsorption isotherm $\pi^S(C)$. Its linearity suggests that the adsorption is of Henry's type, i.e., the adsorbed layer can be considered as being ideal but with adsorption constant larger than that of the gaseous layer. By using this assumption, we analyzed thoroughly the experimental data for 50 systems and obtained reasonable and self-consistent results. This would have been impossible, had the nature of the LE adsorbed layer have been different.

In Sect. 2, we will briefly present a model and an equation for the adsorption constant K_a of nonionic surfactant at liquid interface. This model turns out to be a useful instrument for the analysis of the tensiometric data for these surfactants. In Sect. 3, we present our concept for cohesive and non-cohesive isotherms. The equations of state and the procedures for processing tensiometric data for both types of isotherms are described in Sect. 3.3. In Sect. 4, the dependence of the adsorption constant of cohesive and non-cohesive systems on the surfactant structure and on temperature is interpreted with our model for the adsorption constant. The dependence of the cohesive pressure on the surfactant hydrocarbon chain length is also discussed.

2 Henry's Adsorption Constant, Adsorption Energy and Thickness

2.1 *Henry's Adsorption Isotherm*

Consider an ideal nonionic surfactant solution of concentration C in equilibrium with an ideal gaseous adsorbed monolayer of the same surfactant with adsorption Γ. The surfactant chemical potentials in the two states are

$$\mu^B = \mu_0^B + k_B T \ln C, \tag{1}$$

$$\mu^S = \mu_0^S + k_B T \ln \Gamma. \tag{2}$$

Here superscripts "B" and "S" denote bulk and surface phase, and μ_0^S and μ_0^B are the corresponding standard chemical potentials. At equilibrium, μ^B and μ^S must be equal, which leads to Henry's adsorption isotherm:

$$\Gamma = K_a C, \tag{3}$$

where, the *adsorption constant* K_a of the surfactant in the gaseous adsorption layer is defined by the relation

$$k_B T \ln K_a \equiv \mu_0^B - \mu_0^S. \tag{4}$$

As it is obvious from the derivation, Henry's adsorption isotherm (3) is valid only for adsorption layer consisting of non interacting surfactant molecules, i.e., in a very dilute adsorption layer.

Davies and Rideal [10] proposed the following relation of K_a with the molecular parameters of the surfactant:

$$K_a = \delta_a \exp(E_a/k_BT), \tag{5}$$

where δ_a is referred to as "thickness of the adsorbed layer", and E_a as adsorption energy. They proposed to use for the thickness δ_a the length of the surfactant's hydrophobic tail, an assumption adopted later by others (e.g., [4, 14–16]). For the adsorption energy E_a of surfactants with straight hydrocarbon chain Davies and Rideal used the expression

$$E_a = E_0 + u_{CH_2} n_C. \tag{6}$$

Here n_C is the number of carbon atoms in the hydrophobic chain and u_{CH_2} is the (positive) free energy of transfer of a methylene (-CH_2-) group from the solution into the adsorption layer. E_0 is the n_C-independent part of E_a which was ascribed solely to the adsorption energy E_{head} of the hydrophilic head (cf. (4.3) in [10]). Both assumptions of Davies and Rideal for δ_a and E_a are disputable. More rigorous treatment based on classical statistical thermodynamics was given in [17] based on Gibbs definition of adsorption. We will re-derive the results from [17] using an alternative, quantum mechanical approach.

2.2 *Geometry of a Surfactant Molecule*

A detailed molecular adsorption model should involve the geometrical parameters of the surfactant hydrophobic chain: cross-sectional area $\alpha_\perp$ and length l_{CH_2} per -CH_2- group in the stretched hydrocarbon chain. Therefore, it is pertinent to discuss first their values. The area per molecule of dense-packed molecules, measured in insoluble monolayer of alcohols at the point of collapse, is $18 \pm 0.5 Å^2$ [11, 18]. This is in good agreement with the crystallographic radius of solid alkanes, $18.5 Å^2$ [19, 20]. If at the point of collapse the structure of the dense adsorption layer is hexagonal, the area of collapse must be larger than the actual cross-sectional area $\alpha_\perp$ of the surfactant by a factor of 1.10 (the ratio of the area of a hexagon and the circle inscribed inside it). With this correction, the value $18.5 Å^2$ cited above becomes $\alpha_\perp = 16.5 Å^2$. The corresponding cross-sectional radius is $R_\perp = 2.29 Å$. For the length l_{CH_2} per -CH_2- group of a stretched hydrocarbon chain, the value $1.26 Å$ is accepted [21]. The lateral area (along the chain) per -CH_2- group is then $\alpha_\parallel = 2\pi l_{CH_2} R_\perp = 18.1 Å^2$, which is close to $\alpha_\perp = 16.5 Å^2$.

2.3 *Interaction Potential of a Surfactant Molecule with the Interface*

To evaluate the general expression (4) for K_a, we must find the change in the standard Gibbs free energy of a surfactant molecule when it is transferred from the solution to the interface. The interaction potential $u(z)$ between the surfactant molecule and the interface was modeled by Ivanov et al. [17] by assuming that the surfactant is a solid cylindrical rod, approaching the interface by keeping its normal orientation with respect to it. While its head is at distance $z > n_C l_{CH_2}$, the rod is in the bulk solution and do not interact with the interface (state I in Fig. 1). At $z < n_C l_{CH_2}$, the surfactant penetrates the interface, where according to [17] the following effects contribute to $u(z)$:

- **(i)** When the cap of the hydrocarbon chain touches the surface, a portion of the water|hydrophobic phase interface, of area $\alpha_\perp$, disappears (Fig. 1, state II). The contribution of this process to $u(z)$ was modeled in [17] as a contact potential at $z = n_C l_{CH_2}$:

$$u_{(i)}(z) = \begin{cases} \sigma_0 \alpha_\perp, & z < n_C l_{CH_2}, \\ 0, & z > n_C l_{CH_2}, \end{cases} \tag{7}$$

  where σ_0 is the surface tension of the pure water|hydrophobic phase interface. For water|alkane interface at room temperature, $\sigma_0 \approx 50\,\text{mN/m}$, so the energy $\sigma_0 \alpha_\perp$ is about $2 \times k_B T$, which is by no means negligible. This contribution was first accounted for independently by Ivanov et al. [17] and Kumpulainen et al. [4].
- **(ii)** For the energy u_{CH_3} of transfer of the -CH_3 group, we assume proportionality to the contact area of this group with water [22]. To calculate this area, one can approximate the shape of -CH_3 as a cylinder with a cap. The lateral area of the cylinder is assumed equal to that of a -CH_2- group, $\alpha_\parallel$, and the cap area is assumed equal to the cross-sectional area $\alpha_\perp$ of the hydrocarbon tail. The two areas are almost equal and the energy corresponding to each is $u_{CH_2}\alpha_\parallel$. The energy pertaining to the *cap* only can be represented as a contact potential with the same z-dependence as $u_{(i)}$ in (7):

$$u_{(ii)}(z) = \begin{cases} u_{CH_2}, & z < n_C l_{CH_2}, \\ 0, & z > n_C l_{CH_2}, \end{cases} \tag{8}$$

  The second part of u_{CH_2} (pertaining to the lateral area of -CH_3) is not included in (8); it will be included in the next term, the potential $u_{(iii)}$.
- **(iii)** Assuming for simplicity that the carbon chain remains normal to the interface, one can model the hydrophobic energy due to -CH_2- adsorption (plus the lateral energy of the -CH_3 group) as linear function of the distance z between the surfactant head and the interface:

$$u_{(iii)}(z) = u_{CH_2} z / l_{CH_2}, \qquad n_C l_{CH_2} > z > 0. \tag{9}$$

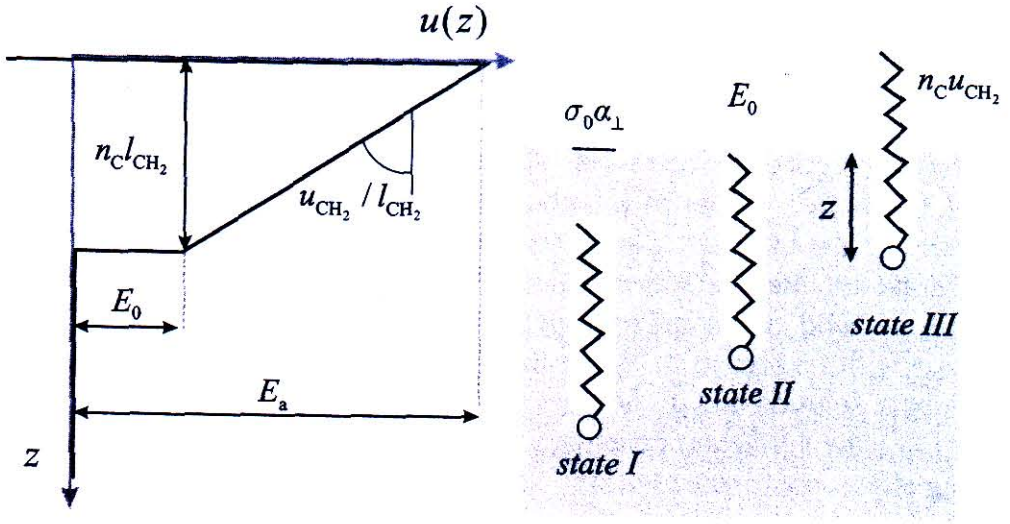

Fig. 1 Molecular interaction potential $u(z)$ of a surfactant molecule with the interface as a function of the distance z between the polar head-group and the interface, cf. (10). According to our model, at distances $z > n_C l_{CH_2}$ (*state I*) there is no significant interaction. At $z = n_C l_{CH_2}$ (*state II*), energy is gained due to the disappearance of clean water surface of area $\alpha_\perp$, and the transfer energy of the cap of the -CH_3 group, cf. (8). At shorter distances (*state III*), there is linear dependence of u on z related to the energy of transfer $n_C u_{CH_2}$ of the hydrocarbon chain from water to the hydrophobic phase, cf. (9)

- **(iv)** Although the hydrophilic head remains immersed in the hydrophilic phase, it also interacts with the interface. This interaction involves probably both short-ranged and long-ranged (such as van der Waals and electrostatic) forces and is strongly specific. Since these forces are not yet fully understood, we will account for their contribution to the adsorption energy E_a by an empirical constant E_{head}.
- **(v)** One finally assumes that the surfactant cannot desorb into the hydrophobic phase, i.e. $u(z) = \infty$ at $z < 0$.

We made above implicitly a simplification of the stage of the penetration of the interface by the -CH_3 group. In fact, stages **(i)** and **(ii)** above cannot be separated. They are part of a continuous process starting in the moment when the -CH_3 group touches the interface and ending when the whole group is in the hydrophobic phase. It is hardly possible to describe correctly this process at least because the exact geometry of the -CH_3 group is unknown. That is why we used the approximate model described in paragraphs **(i)** and **(ii)** above.

Combining the contributions **(i)–(v)**, one obtains an approximate expression for the interaction potential of a surfactant molecule with the interface [17] (see Fig. 1):

$$u(z) = \begin{cases} \infty & 0 > z, \\ -E_a + u_{CH_2} z / l_{CH_2}, & n_C l_{CH_2} > z > 0, \\ 0, & z > n_C l_{CH_2}, \end{cases} \tag{10}$$

where the adsorption energy E_a is given by

$$E_a = E_{head} + \alpha_\perp \sigma_0 + u_{CH_2}(n_C + 1). \tag{11}$$

In (10), the free energy of the surfactant in the bulk solution is used as reference state. Comparison of (11) and (6) leads to an explicit expression for the empirical constant E_0 of Davies and Rideal [10]:

$$E_0 = E_{head} + u_{CH_2} + \alpha_\perp \sigma_0. \tag{12}$$

It encompasses not only E_{head} as assumed by Davies and Rideal, but also the other contributions to E_a, unrelated to the adsorption of the -CH_2- chain (namely, $u_{CH_2} + \alpha_\perp \sigma_0$).

2.4 *Partition Functions of a Surfactant Molecule at the Interface*

We will account now for the effects of the kinetic energies on the adsorption by investigating the partition function of the surfactant molecule at the interface. We use the model (10) for the interaction potential $u(z)$. Since the "width" of the potential well is very small (in fact zero as z goes to zero), one might expect quantum mechanical effects to play certain role for the value of K_a. Therefore, we adopt a quantum mechanical approach to the problem.

Let us denote the energies of interaction of the surfactant molecule with the medium in the bulk and at the surface by u^B and u^S respectively (with account to Fig. 1, $u^B - u^S = E_a$). For ideal systems one can deduce the standard chemical potentials in the bulk and at the surface, μ_0^S and μ_0^B from Eqs. (4.26) and (7.8) of Hill [23]:

$$\mu_0^B = u^B - k_B T \ln q_{trans}^B - k_B T \ln q_{rot}^B, \tag{13}$$

$$\mu_0^S = u^S - k_B T \ln q_{trans}^S q_{vibr,z}^S - k_B T \ln q_{rot}^S, \tag{14}$$

where q^B and q^S are the respective quantum partition functions. We account for the translational and rotational degrees of freedom in the bulk and at the surface (indicated with subscript), and for the partition function $q_{vibr,z}^S$ standing for the vibration of the molecule at the surface in the potential well defined by $u(z)$, (10).

- **(i)** *Translational degrees of freedom.* A surfactant molecule in the bulk moves freely in 3 directions, while at the surface transition is possible only in x and y directions. Therefore,

$$q_{trans}^B = \Lambda^{-3}, \qquad q_{trans}^S = \Lambda^{-2}, \tag{15}$$

where $\Lambda = h/(2\pi m k_B T)^{1/2}$ is de Broglie thermal wavelength [23], m is molecular mass and h is Planck constant.

- **(ii)** *Vibration in z direction.* For the potential in Fig. 1, the surfactant molecules oscillate in a triangular potential well:

$$u(z) = \begin{cases} u_{CH_2} z / l_{CH_2}, & z > 0, \\ \infty, & z < 0. \end{cases} \tag{16}$$

For vibrations in such potential, one can apply the Wentzel–Kramers–Brillouin approximation [24] for the energies ϵ_ν of the quantum states with quantum numbers $\nu = 1 \div \infty$:

$$\epsilon_\nu = \epsilon_1 \left(\frac{4\nu - 1}{3} \right)^{2/3}, \tag{17}$$

where the energy of the basic state ϵ_1 is given by

$$\epsilon_1 = \frac{3^{4/3} h^{2/3}}{8 m^{1/3}} \frac{u_{CH_2}^{2/3}}{l_{CH_2}^{2/3}}. \tag{18}$$

If $\epsilon_1 \ll k_B T$, the Euler's summation formula can be used to calculate the partition function $q^S_{vibr,z}$ (e.g. (44.5) and (44.6) in the book of Levich [25]):

$$q^S_{vibr,z} \equiv \sum_{\nu=1}^{\infty} \mathrm{e}^{-\epsilon_\nu / k_B T} \approx \int_1^{\infty} \mathrm{e}^{-\epsilon_\nu / k_B T} \mathrm{d}\nu + \frac{1}{2} \mathrm{e}^{-\epsilon_1 / k_B T}. \tag{19}$$

The integral in the right side can be taken analytically. Thus one obtains:

$$q^S_{vibr,z} = \frac{9\sqrt{\pi}}{16} \left(\frac{\epsilon_1}{k_B T} \right)^{-3/2} \left(1 + \sqrt{\frac{4}{\pi} \frac{\epsilon_1}{k_B T}} \mathrm{e}^{-\epsilon_1 / k_B T} - \mathrm{erf} \sqrt{\frac{\epsilon_1}{k_B T}} \right) + \frac{1}{2} \mathrm{e}^{-\epsilon_1 / k_B T}, \tag{20}$$

where "erf" is the error function. By taking now the limit $\epsilon_1 \ll k_B T$ one obtains

$$q^S_{vibr,z} = \frac{k_B T}{\Lambda} \frac{l_{CH_2}}{u_{CH_2}} - \frac{1}{4}. \tag{21}$$

The first term in the right hand side of (21) coincides with the result of Ivanov et al. [17] obtained by classical mechanical derivation and Gibbs' definition of adsorption. The 1/4 is a quantum mechanical correction. For a hydrocarbon chain at water|oil interface (W|O), $u_{CH_2} = 1.39 \times k_B T$ [21] and the value of the first term is about 12 for hexanol at 25°C. Therefore, the quantum correction is typically less than 2% and can be neglected. Then,

$$q^S_{vibr,z} = \frac{k_B T}{\Lambda} \frac{l_{CH_2}}{u_{CH_2}}. \tag{22}$$

This justifies the classical derivation of the adsorption constant K_a in Ref. [17].

- **(iii)** *Rotation.* In order to estimate the contribution of the rotation to the adsorption constant K_a, it is sufficient to calculate the partition functions for the initial (in the bulk) and the final (at the surface) states. For simplicity we will assume that the molecule rotates as a solid stick of inertial moment I. The Hamiltonian of a freely rotating stick in spherical coordinates (r, ϑ, φ) is [23]:

$$H = \frac{1}{2I}\left(p_\vartheta^2 + p_\varphi^2/\sin^2\vartheta\right).$$

Here p_ϑ and p_φ are the corresponding momenta of the stick. This corresponds to bulk partition function ((8)–(27) of [23]):

$$q_{rot}^B = \frac{1}{h^2}\int_{-\infty}^{\infty}\int_{-\infty}^{\infty}\int_0^{\pi}\int_0^{2\pi} \mathrm{e}^{-H/k_BT}\mathrm{d}\varphi\mathrm{d}\vartheta\mathrm{d}p_\varphi\mathrm{d}p_\vartheta = 8\pi^2 k_B T I/h^2. \quad (23)$$

We will assume also that the rotation of the surfactant at the interface $z = 0$ is again free but restricted to the semi-space $z < 0$. This yields for the surface partition function q_{rot}^S:

$$q_{rot}^S = \frac{1}{h^2}\int_{-\infty}^{\infty}\int_{-\infty}^{\infty}\int_0^{\pi/2}\int_0^{2\pi} \mathrm{e}^{-H/k_BT}\mathrm{d}\varphi\mathrm{d}\vartheta\mathrm{d}p_\varphi\mathrm{d}p_\vartheta = 4\pi^2 k_B T I/h^2. \quad (24)$$

- **(iv)** It is difficult to calculate the contribution of all intramolecular vibrational and rotational states to the adsorption constant K_a. We believe, however, that they are implicitly accounted for in the empirical values of the transfer energy u_{CH_2} and in the constant E_{head} in (12).

Substituting the results (15), (22)–(24) into the expressions (13) and (14) for the standard chemical potentials, we obtain

$$K_a \equiv \exp\frac{\mu_0^B - \mu_0^S}{k_BT} = \frac{k_BT l_{CH_2}}{2u_{CH_2}}\exp\frac{E_a}{k_BT}. \quad (25)$$

Comparison with (5) yields for the adsorption thickness δ_a the expression

$$\delta_a = \frac{k_BT}{2}\frac{l_{CH_2}}{u_{CH_2}}. \quad (26)$$

This differs from the corresponding expression in [17] with the factor 1/2 originating from (24) for q_{rot}^S. With the values $l_{CH_2} = 1.26\text{Å}$ and $u_{CH_2}^{WO} \approx 1.39k_BT$ (cf. [21] and Sect. 4.2 below), one obtains for simple surfactants at W|O $\delta_a = 0.45\text{Å}$. For water|gas surface (W|G), $u_{CH_2}^{WG} \approx 1.04k_BT$, so that the adsorption thickness is higher: $\delta_a = 0.63\text{Å}$. These values of δ_a are quite different from those based on the assumption of Davies and Rideal that δ_a is

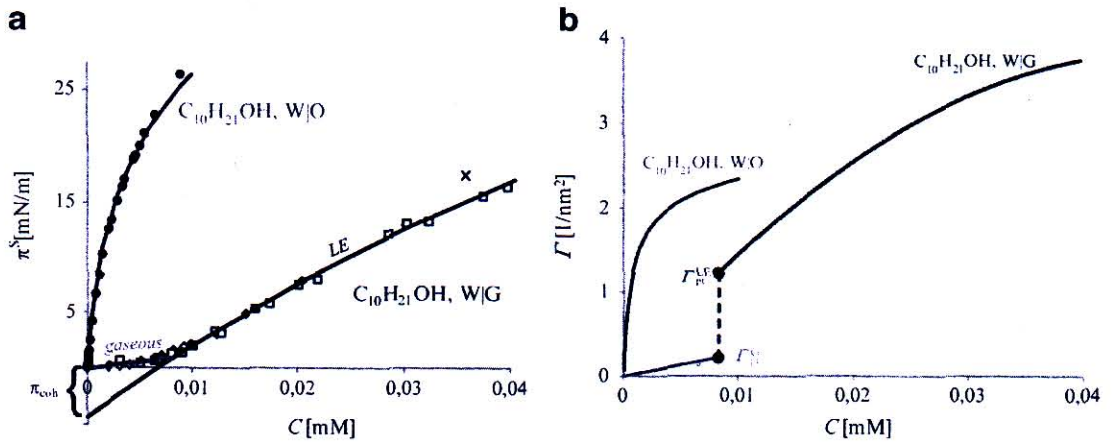

Fig. 2 (**a**) Surface pressure isotherm (π^S vs. C) of $C_{10}H_{21}OH$ at W|dodecane and W|G interfaces. At W|G, the decanol behaves as a cohesive surfactant and demonstrates $\pi^S(C)$ isotherm of LE-type. The LE line is a regression with quadratic polynomial with non-zero intercept, cf. (32). In the Henry region, (30) is followed, indicating gaseous state of the monolayer. At W|O the same surfactant follow the HFL isotherm with $\alpha = 16.5\,Å^2$. Adsorption constant was the only fitting parameter ($K_a = 6.54 \times 10^{-3}$ m). (**b**) The corresponding adsorption isotherms, $\Gamma(C)$, obtained as $\Gamma = \mathrm{d}\pi^S/\mathrm{d}k_BT\ln C$. Marked by dots are the points of phase transition of the gaseous and the LE phase (Γ_{pt}^G and Γ_{pt}^{LE} respectively)

equal to the length of the hydrophobic chain (e.g., for dodecanol they recommend $\delta_a = 12 \times l_{CH_2} = 15\,Å$)

3 Cohesive and Non-cohesive Adsorption of Surfactants

We analyzed numerous experimental data for surface pressure $\pi^S(= \sigma_0 - \sigma)$ vs. concentration C and found that at low concentrations virtually all of them exhibit one of two distinctive types of behavior. In some cases (Fig. 2a, line W|O), the plot starts with a linear section with zero intercept. In other cases (Fig. 2a, lines W|G) there are two sections: one with intercept zero and a second one having finite negative intercept ($-\pi_{coh}$), the two region divided by a distinctive kink. For reasons, which will become clear in this section, we will call the first type of adsorption behavior *non-cohesive*, and the second one *-cohesive*.

3.1 Non-cohesive Adsorption and Helfand–Frisch–Lebowitz Model

The governing molecular property of the surfactant in the non-cohesive case is its actual molecular area α (i.e., the effective cross-sectional area, cf. Sect. 2.2).

The most widely used models for non-cohesive adsorption of surfactants at liquid surfaces are the Langmuir model (rigorously valid only for localized adsorption at solid surfaces [23,26]) and Volmer model (which is in fact the exact solution of the problem for one-dimensional fluid of rods [27,28] but not for adsorption of circular discs at planar interface). A more natural model for the non-cohesive adsorption layer of small molecules seems to be a two-dimensional fluid of hard discs. A nearly exact surface equation of state (EOS) of this system was derived by Helfand, Frisch and Lebowitz (HFL) [29,30]:

$$\frac{\pi^S}{k_B T} = \frac{\Gamma}{(1-\alpha\Gamma)^2}. \tag{27}$$

From (27), the dependence of the chemical potential μ^S of the surfactant at the interface on the adsorption Γ can be obtained by integration of the Gibbs isotherm, $\mathrm{d}\pi^S = \Gamma \mathrm{d}\mu^S$. This yields:

$$\mu^S = \mu_0^S + k_B T \ln \gamma^S \Gamma, \qquad \ln \gamma^S = -\ln(1-\alpha\Gamma) + \frac{\alpha\Gamma(3-2\alpha\Gamma)}{(1-\alpha\Gamma)^2}. \tag{28}$$

Here γ^S is the surface activity coefficient. The condition $\mu^S = \mu_0^S + k_B T \ln \Gamma$ at $\Gamma \to 0$ was used for the determination of the integration constant. The adsorption isotherm $\Gamma(C)$ corresponding to HFL model follows from the equilibrium condition $\mu^S = \mu^B$, where μ^S is given by (28) and the chemical potential of the surfactant in an ideal bulk solution is $\mu^B = \mu_0^B + k_B T \ln C$; the result is:

$$K_a C = \frac{\Gamma}{1-\alpha\Gamma} \exp\left[\frac{\alpha\Gamma(3-2\alpha\Gamma)}{(1-\alpha\Gamma)^2}\right]. \tag{29}$$

For non-ideal bulk solution, the concentration C in (29) must be replaced with activity γC, where γ is the bulk activity coefficient. The adsorption isotherm (29) was derived first by Ivanov et al. [17] (Helfand et al. derived in fact only the EOS (27) [29]), but since (29) is based on HFL model, we will still call it "HFL adsorption isotherm". Equations (27) and (29) define parametrically the surface tension isotherm $\pi^S(C)$ (with parameter Γ). When both (27) and (29) are used for the interpretation of $\pi^S(C)$ data, we will term their combination "HFL model".

The HFL model is suitable especially for the case of adsorption at W|O, where attraction between hydrocarbon chains is known [9,22] to be very small. We will show below that non-cohesive behavior is not rare also at W|G, although there is no guarantee that attractive interaction is completely absent in this case. Nevertheless, we will use (27) and (29) for non-cohesive surfactants at W|G as a tool for analysis of their adsorption constant K_a. At that, we will obtain also values of the actual molecular area α, but will not analyze them since it is possible that they depend significantly on the neglected attractive interactions.

3.2 Cohesive Adsorption: Phenomenological Relations

As already mentioned, a typical feature of the cohesive isotherms is the existence of a kink in the $\pi^S(C)$ isotherm at low concentration (cf. Fig. 2, octanol at W|G). The lack of such kink is indicative of non-cohesive adsorption (cf. Fig. 2, octanol at W|O). Henry's region before the kink corresponds to gaseous state of the monolayer. The behavior right after the kink is close to linear, with negative intercept, $-\pi_{coh}$. Cohesive adsorption behavior was discovered by Adam [1,3] who noticed that, with insoluble surfactants, between the gaseous and solid-like state of the adsorption layer, a state with intermediate compressibility occurs. He called it "liquid expanded (LE) state". Langmuir showed that the quantitative interpretation of the experimental EOS needs the introduction of a negative surface pressure, which he called "spreading pressure" [2]. Although our analysis of the adsorption behavior of soluble surfactants is rather different from that of Langmuir, we will still call the adsorption layer "liquid expanded", but we will use for the negative intercept the notion cohesive pressure π_{coh} introduced by Davies [9, 10].

3.3 Processing of Experimental Data

Since the data interpretation in the two cases (cohesive and non-cohesive) involves a number of steps, we will now illustrate in details the computational procedures on the examples in Fig. 2, decanol at W|G and W|octane.

a. Non-cohesive Adsorption

The interfacial tension data of Aveyard and Briscoe [31] for fatty alcohols at W|O interface were presented by the authors as function of the concentration C^O of the surfactant in the oil phase, where the alcohols are more soluble. In order to be able to compare the adsorption in these systems with adsorption at W|G, we recalculated the corresponding concentration C^W of octanol in the water by using the equilibrium condition $C^W = \gamma^O C^O / K_p$, where K_p is the partition coefficient. The activity coefficient γ^O cannot be neglected for the alkane solutions, as they were concentrated and alcohols are known to tetramerize in oil solutions [32]. For dodecanol in octane at 30°C the tetramerization constant is $K_{1,4} = 780M^{-3}$ [32]. We assumed that this value is valid for all considered alcohol solutions in alkanes, since the tetramerization is probably determined by the interaction between the hydrophilic heads. The activity coefficient γ^O was calculated by solving the equation $C^O = \gamma^O C^O + 4K_{1,4}\left(\gamma^O C^O\right)^4$ following from the monomer–tetramer model [32]. The partition coefficient for the transfer of a surfactant molecule from oil to water follows an exponential dependence on n_C [33]. Data for alcohols are concordant with the equation $\ln K_p = -4.90 + 1.31 \times n_c$ ($K_p = 3,700$ for decanol

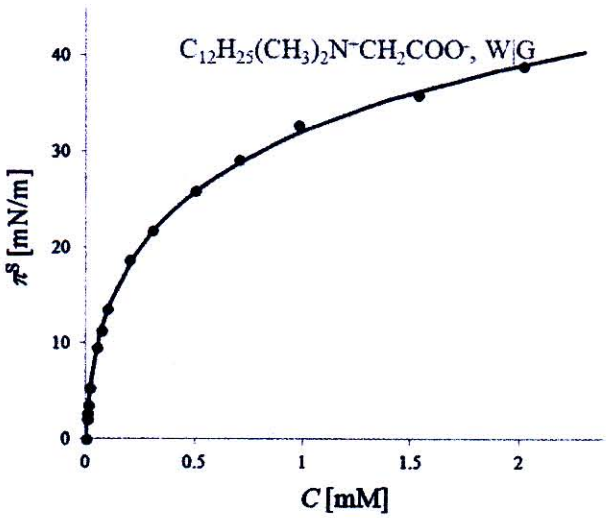

Fig. 3 Surface pressure isotherm (π^S vs. C) of $C_{12}H_{25}Me_2N^+CH_2COO^-$ at W|G interface. An example for non-cohesive isotherm at W|G. Line: HFL isotherm according to (27) and (29) with $\alpha = 19.6 Å^2$ and $K_a = 1.83 \times 10^{-4}$ m. Experimental data is from [34]

in Fig. 2a). The so-obtained π^S vs. C^W data are perfectly fitted by the HFL model (line "W|O" in Fig. 2a), by using fixed actual molecular area $\alpha = 16.5 Å^2$ of the hydrocarbon chain. The adsorption constant K_a is the only free parameter in (27) and (29): $K_a = 6.54 \times 10^{-3}$ m. The K_a values, determined by such one-parametric fit, have a very small error (less than 1% for ln K_a).

Only surfactants of relatively large head-groups follow non-cohesive behavior at W|G. In the cases of non-cohesive adsorption at W|G, the data processing does not require calculation of activities, as all investigated solutions were diluted (Fig. 3). Unlike the case of alcohols at W|O, for surfactants at W|G there is no independent source of information for α. Besides, it is not certain that HFL model is exact in this case since the disregarded intermolecular attraction may affect the value of the α-parameter of HFL. Therefore, we could not use the HFL model with only one parameter as it was with W|O, and instead we determined both K_a and α as adjustable parameters at W|G. The typical error in the values of these two parameters is $\pm 7\%$ for ln K_a and $\pm 2 Å^2$ for α in cases when sufficient experimental data are disposable. The errors could be even higher (up to $\pm 20\%$ for ln K_a) when no measurements in the low-concentration region are available (this is usually the case).

b. Cohesive Adsorption

The W|G data in Fig. 2, which are typical example for cohesive adsorption, refer again to adsorption of decanol. Before the kink, a close-to-linear dependence of π^S on C without intercept is observed. This is the gaseous region, which is treated by using the Henry's EOS, cf. (3):

$$\pi^S = k_B T K_a^G C_s. \tag{30}$$

The data in the gaseous region are scarce and rather scattered; therefore, ln K_a^G is determined with a high error, $\pm 10\%$ at best.

After the kink, at intermediate concentrations, a second region is observed (Fig. 2). Some measurements exhibit in this region enough experimental points to depict a well-defined linear dependence $\pi^S(C)$, but with negative intercept [4]. Denoting this intercept by π_{coh}, one can write the following surface pressure isotherm for this linear region:

$$\pi^S = -\pi_{coh} + k_B T K_a^{LE} C. \tag{31}$$

In cases when the experimental data are scarce or scattered and the linear region is not well visible, we preferred use a square polynomial fit (LE curve in Fig. 2) with the equation:

$$\pi^S = -\pi_{coh} + k_B T K_a^{LE} C + k_B T B_2 \left(K_a^{LE}\right)^2 C^2, \tag{32}$$

which is, in fact, a virial expansion of the surface pressure isotherm (B_2 is the second virial coefficient). We believe that when the quadratic fit with (32) of given set of surface tension data yields a negative intercept $-\pi_{coh}$, the respective surfactant forms a *liquid expanded* layer. The value of $\ln K_a^{LE}$ determined by this fit is typically with error of the order of $\pm 15\%$. The accuracy of the π_{coh} value is also $\pm 15\%$. However, sometimes the error of π_{coh} can be due, at least in part, to systematic error of the surface tension measurements (cf. [6] for discussion).

From the phenomenological surface pressure isotherms (30) and (32), and the Gibbs isotherm one can calculate the respective adsorption isotherms of the gaseous and the LE state:

$$\Gamma = K_a^G C \quad \text{for gaseous state,} \tag{33}$$

$$\Gamma = K_a^{LE} C + 2B_2 \left(K_a^{LE}\right)^2 C^2 \quad \text{for LE state.} \tag{34}$$

In Fig. 2b, the isotherms (33) and (34) for $C_{10}H_{21}OH$ at W|G are plotted along with the result obtained for the same surfactant at W|O by means of HFL adsorption isotherm (29). The adsorption parameters for this plot were determined from the $\pi^S(C)$ data in Fig. 2a. The break of the curve $\Gamma(C)$ corresponds to phase transition from gaseous to LE state (dashed line in Fig. 2b).

4 Analysis of the Experimental Data for the Cohesive Pressure π_{coh} and the Adsorption Constant K_a

Let us now consider the experimental results for the adsorption of some homologous series of nonionic surfactants, analyzed in the framework of the ideas presented in the previous Sects. 2 and 3. We have processed the tensiometric data for 46 nonionic surfactants from nine homologous series at different interfaces and conditions (Fig. 6; cf. "List of symbols and abbreviations" (Table 1) for surfactants' names).

Table 1 List of symbols and abbreviations

B_2	Second virial coefficient
C	Surfactant concentration in the aqueous solution
E_a	Adsorption energy
E_{head}	Energy of transfer of surfactant's head from the bulk to the interface
k_B	Boltzmann constant
K_a	Henry's adsorption constant ($\Gamma = K_a C$)
l_{CH_2}	Length per -CH_2- group (1.26 $\AA$)
n_C	Number of carbon atoms in surfactant's hydrophobic chain
q	Partition function
T	Temperature
u_{CH_2}	Free energy for transfer of -CH_2- from water to hydrophobic phase
z	Cartesian coordinate
α	Actual area of a molecule
β	Attraction parameter
γ	Activity coefficient
Γ	Surfactant adsorption
δ_a	Adsorption thickness
μ	Chemical potential
π_{coh}	Cohesive pressure
π^S	Surface pressure, $\pi^S = \sigma_0 - \sigma$
σ	Surface tension
σ_0	Surface tension of the pure interface in the absence of surfactant
2D	Two-dimensional
cmc	Critical micelle concentration
EOS	Equation of state
HFL	Helfand–Frisch–Lebowitz model
LE	Liquid expanded state of the adsorption layer
W|G	Water–gas interface
W|O	Water–oil interface
-CH_2-	Methylene group
-CH_3-	Methyl group
$C_nH_{2n+1}OH$	Alkan-l-ol
$C_{n-1}H_{2n-1}COOH$	Alkanoic acid
$C_nH_{2n+1}Me_2PO$	An-alkyl dimethyl phosphine oxides
$C_8H_{17}SOC_2H_4OH$	Octylsulfinylethanol
$C_{10}H_{21}Mal$	n-Decyl β-maltopyranoside
$C_{10}H_{21}Glu$	n-Decyl β-glucopyranoside
$C_{10}H_{21}SMal$	n-Decyl β-D-thiomaltopyranoside
$C_nH_{2n+1}Me_2N^+CH_2COO^-$	N-n-alkyl-N, N-dimethylglycine
$C_8H_{17}PEM$	Maleic acid mono [2-(4-n-alkylpiperazinyl)ethyl ester]

All investigated surfactants ($C_nH_{2n+1}OH$) display at W|O non-cohesive adsorption behavior. There are some surfactants, mainly with short hydrocarbon chains and bulky head-groups ($C_nH_{2n+1}Me_2N^+CH_2COO^-$, short-chain $C_nH_{2n+1}Me_2PO$ etc.), which behave non-cohesively even at W|G interface. Cohesive (LE) type of surface pressure isotherms were found with most surfactants at W|G, like $C_{n-1}H_{2n-1}COOH$ at low pH, $C_nH_{2n+1}OH$, long-chained $C_nH_{2n+1}PEM$. Moreover, two homologous series of surfactants, $C_nH_{2n+1}Me_2PO$ and $C_nH_{2n+1}Me_2PEM$, exhibit transition from non-cohesive to cohesive behavior with the increase of the hydrocarbon chain length: for the W|G adsorption layers of $C_nH_{2n+1}Me_2PO$ with $n_C = 8 \div 10$ there is no LE region, while the homologues with $n_C = 11 \div 15$ exhibit gaseous-LE phase transition. The behavior of $C_nH_{2n+1}PEM$ is similar to that of $C_nH_{2n+1}Me_2PO$: $n_C = 8$ is non-cohesive, $n_C = 9 \div 11$ are cohesive.

4.1 The Cohesive Pressure π_{coh}

We will base our interpretation of the cohesive isotherms and the phenomenological equations (31) and (32) on Langmuir's concept for liquid expanded monolayer [2]. Langmuir's idea for the origin of the intercept $-\pi_{coh}$ (e.g. [3]) can be quantified as follows. Let σ_0^{WO} be the interfacial tension of the pure W|O interface, and σ_0^{OG} be the oil|gas surface tension. The surfactant hydrophobic tails are adsorbed at the W|G interface and form a structureless oil-like film whose total tension must be $\sigma_0^{WO} + \sigma_0^{OG}$. The hydrophilic heads are adsorbed at the W|O interface of this oil film. In the initial part of the LE region of the dependence π^S vs. C, the "adsorption" of the heads must be ideal. Then, one can write for the tension of the adsorption layer [4]

$$\sigma = \sigma_0^{OG} + \sigma_0^{WO} - k_B T K_a^{LE} C. \tag{35}$$

Here, the last term, stemming from (3), is due to (ideal) adsorption of surfactant's hydrophilic heads. However, by definition, the surface pressure at W|G is $\pi^S = \sigma_0^{WG} - \sigma$. Inserting here σ from (35), and comparing the result with (31), one obtains

$$\pi_{coh} = \sigma_0^{WO} + \sigma_0^{OG} - \sigma_0^{WG} \tag{36}$$

According to these simple considerations, the intercept $-\pi_{coh}$ coincides with the spreading coefficient of a hydrocarbon on water [2]. Therefore, the negative cohesive pressure $-\pi_{coh}$ was at first referred to as *spreading pressure*; the term "cohesive pressure" was introduced by Davies [9].

The simple considerations above give correctly only the order of the value of π_{coh}, but in fact they cannot explain the dependence of π_{coh} on the surfactant tail-length and head-group. The experimental dependence of π_{coh} on n_C is plotted in Fig. 4. The cohesive pressure increases with e.g. $\Delta\pi_{coh} = 0.7$ mN/m per -CH_2- group. This increment corresponds to surface energy per -CH_2- group equal to $\alpha_\perp \Delta\pi_{coh} \approx k_B \times 8$, in good agreement with the experimental finding that "the effect of each additional CH_2 group in the chain is equivalent to a lowering of

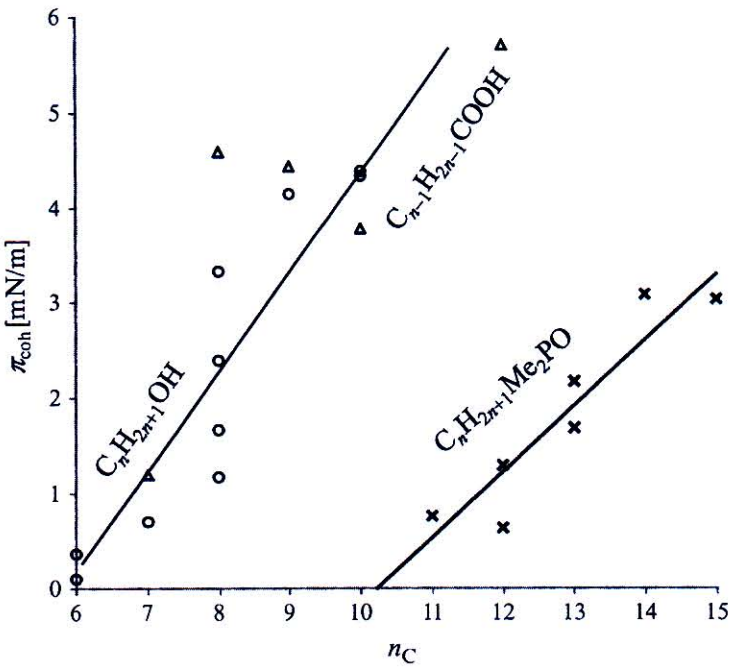

Fig. 4 Dependence of the cohesive pressure π_{coh} on hydrocarbon chain-length n_C for 3 homologous series: alkanols (*circles*), alkanoic acids (*triangles*) and alkyldimethyl phosphine oxides (*crosses*). The dependence is close to linear. For $C_nH_{2n+1}Me_2PO$, the value of n_C at which $\pi_{coh} = 0$ corresponds well with the transition length at which this homologous series becomes non-cohesive: the isotherm of $C_{10}H_{21}Me_2PO$ has no LE region. Tensiometric data from [35–37] were used to calculate π_{coh}

temperature of about 8°C" [2]. It is remarkable that the transition from cohesive to non-cohesive behavior of $C_nH_{2n+1}Me_2PO$ coincides with the value of n_C at which π_{coh} becomes zero (n_C between 10 and 11: $C_{11}H_{23}Me_2PO$ forms cohesive layers and $C_{10}H_{21}Me_2PO$ is non-cohesive). With alkanols and alkanoic acids, the values of π_{coh} are rather uncertain due to the insufficient experimental data. However, their behavior appears to be similar. One can predict from Fig. 4 that pentanol and pentanoic acid will form non-cohesive monolayers.

4.2 *Effect of the Surfactant Structure on the Adsorption Constant K_a*

The data for non-cohesive adsorption of $C_nH_{2n+1}OH$ ($n_C = 8 \div 18$) at W|O (oil phases are various alkanes) were processed by means of HFL model, (27) and (29), with $\alpha = 16.5\,\text{Å}^2$, as explained in Sect. 3. The adsorption constant K_a was the only free adjustable parameter. The dependence of $\ln K_a$ on n_C is shown in Fig. 5. It is linear with slope $u_{CH_2}/k_BT = 1.39$, corresponding to the known energy of transfer from water to oil phase [21]. For non-cohesive adsorption at W|G interface, again HFL model was used, but with two free parameters, α and K_a. The values obtained for α depend only on the head-group of the surfactant:

$$C_nH_{2n+1}Me_2N^+CH_2COO^- \quad \text{with} \quad n_C = 8 \div 16 : \alpha = 18.8 \pm 1.5\text{Å}^2,$$
$$C_nH_{2n+1}Me_2PO \quad \text{with} \quad n_C = 8 \div 10 : \qquad \alpha = 22 \pm 1\text{Å}^2,$$
$$C_8H_{17}PEM : \qquad \alpha = 25\text{Å}^2.$$

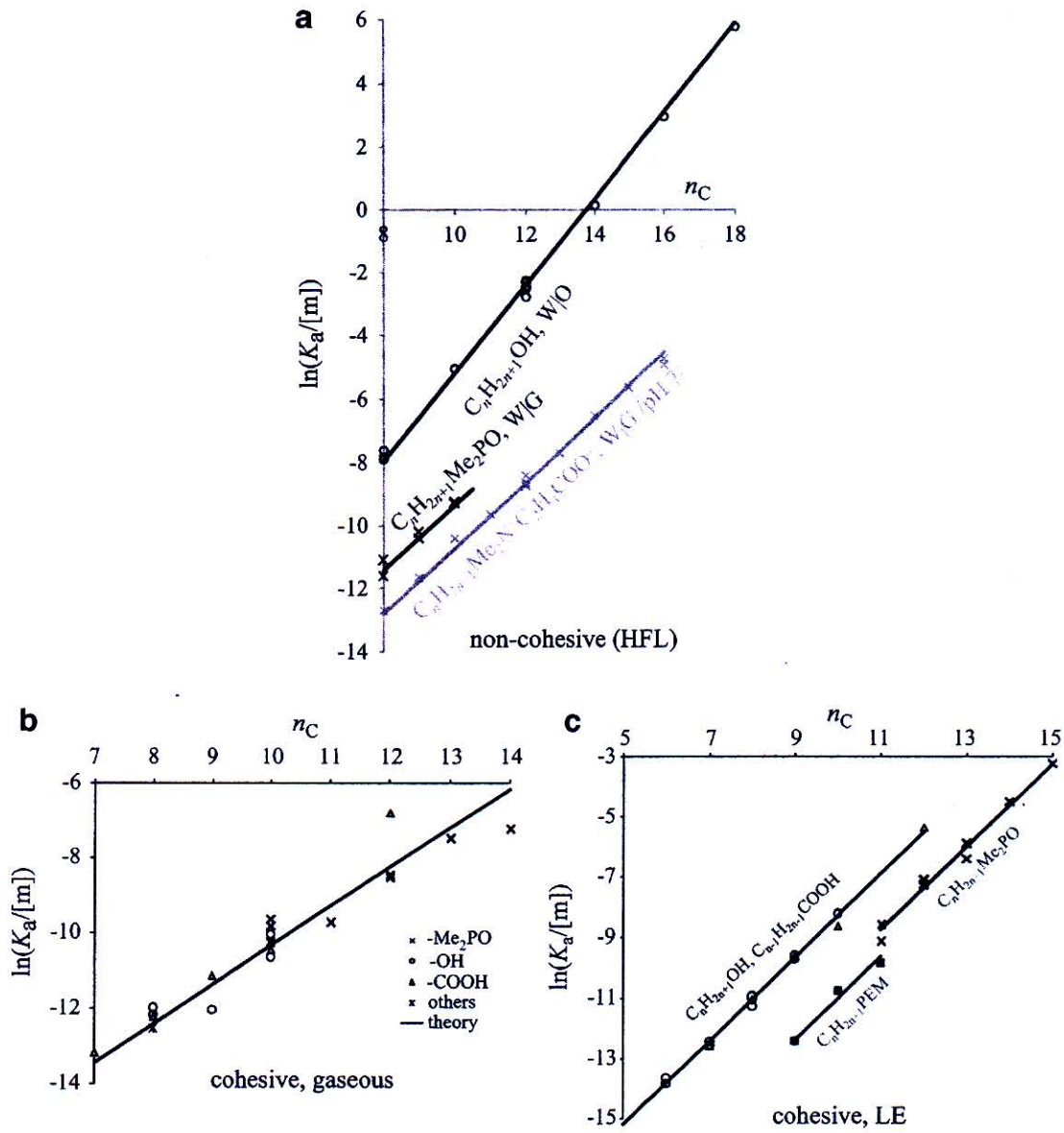

Fig. 5 Dependence of the logarithm of the adsorption constant $\ln K_a$ on the chain length n_C. (**a**) Non-cohesive adsorption: results from fit of tensiometric data with HFL model (similar to the fits in Figs. 2a and 3). The *lines* represent fits with (37) with fixed slopes ($u_{CH_2}/k_BT = 1.39$ for W|O and 1.04 for W|G data). (**b**) Cohesive adsorption, gaseous region. All data fall on a single line with slope 1.04 and intercept $\ln(K_a^\circ/[m]) = -20.7$, cf. (37). (**c**) Cohesive adsorption, LE-region. Lines are fits with fixed slopes, 1.39. Data for alkanoic acids at low pH and alkanols fall on a single curve with intercept −22.2, while the intercepts for $C_nH_{2n+1}Me_2PO$ and $C_nH_{2n+1}PEM$ are significantly smaller. The tensiometric data used is from different sources (cf. Fig. 6 for the complete list)

In contrast to $C_nH_{2n+1}OH$ at W|O, the linear dependence of $\ln K_a$ on n_C for $C_nH_{2n+1}Me_2N^+CH_2\,COO^-$ and $C_nH_{2n+1}Me_2PO$ at W|G has slope $u_{CH_2}/k_BT = 1.04$ (Fig. 5a), typical for the transfer of a methylene group from water to gas [21].

Cohesive surface tension isotherms are observed only at W|G. Data for $C_nH_{2n+1}OH$, $C_{n-1}H_{2n-1}COOH$, long-chained $C_nH_{2n+1}Me_2PO$ and $C_nH_{2n+1}PEM$,

$C_8H_{17}SOC_2H_4OH$, $C_{10}H_{21}SMal$, $C_{10}H_{21}Mal$ and $C_{10}H_{21}Glu$ were processed. The experimental data for $\ln K_a^G$ vs. n_C for the gaseous region of all these surfactants fall on a single straight line with slope $u_{CH_2}/k_BT = 1.04$ (Fig. 5b), and with intercept $\ln(K_a^o/[m]) = -20.7$. The LE region was processed with (32). With all these surfactants, the slope of the dependence of $\ln K_a^{LE}$ on n_C is $u_{CH_2}/k_BT = 1.39$ (Fig. 5c), i.e., the same as for the adsorption at W|O interface. This is certainly due to the fact that the transfer of -CH_2- is from water to LE adsorption layer, i.e., into an oil-like environment. The value of the intercept $\ln K_a^\circ$ of this dependence is the same for $C_nH_{2n+1}OH$ and $C_{n-1}H_{2n-1}COOH$. However, the $C_nH_{2n+1}Me_2PO$ have significantly lower values of $\ln K_a^\circ$ than the corresponding acids and alcohols, and with $C_nH_{2n+1}PEM$, $\ln K_a^o$ is even smaller (Fig. 5).

We now turn to the interpretation of the value of the intercepts $\ln K_a^\circ$ of the lines in Fig. 5. To compare the statistical model of K_a to the experimental data in Fig. 5, it is convenient to represent (5), (11) and (26) in logarithmic form:

$$\ln K_a = \ln K_a^\circ + n_C u_{CH_2}/k_BT, \tag{37}$$

where the intercept $\ln K_a^\circ$ of the experimental dependence of $\ln K_a$ on n_C is given by

$$\ln K_a^\circ \equiv \ln \delta_a + (E_{head} + u_{CH_2} + \alpha_\perp \sigma_\perp)/k_BT. \tag{38}$$

Here δ_a is the adsorption length, (26). The experimental value of the intercept $\ln K_a^\circ$ can be determined directly when data for several members of a homologous series are available (cf. Fig. 5). However, in few cases (e.g. for $C_8H_{17}SOC_2H_4OH$, $C_{10}H_{21}Mal$ etc.), data were available only for a single surfactant. Then, $\ln K_a^\circ$ was calculated from (37) with the known value of u_{CH_2}/k_BT (1.39 or 1.04) and the experimental $\ln K_a$ for this surfactant. The results for $\ln K_a^\circ$ for nine homologous series are presented in Fig. 6. The following comments of these results seem pertinent:

- 1. For all non-cohesive surfactants at W|G and for the gaseous region of all cohesive surfactants, the difference between theoretical and experimental values of $\ln K_a^\circ$ is about u_{CH_2}/k_BT (cf. Fig. 6). One possible reason for this difference is that the first carbon atom from the hydrocarbon tail is immersed in the water—that is why we called it "immersion energy". Such position of the surfactant molecule is natural for -COOH, where there is one C-atom in the carboxylic group. For the other examples in the Fig. 6, the immersion of the first C-atom might be due to the interaction of the head-group with the interface, i.e. to the neglected term E_{head} in (38). The analysis of this effect is complicated and will be postponed to a subsequent publication.
- 2. The comparison of the experimental and theoretical values of K_a in the LE region for the surfactants in Fig. 6 at W|G was done with intercept $\ln K_a^\circ$ calculated with $\sigma_0 = 50$ mN/m instead of 72.2 mN/m, as if the surfactant adsorbs at W|O interface. This in accord with Langmuir's interpretation of LE state.

surfactant, number of C-atoms, interface[a]	$\ln(K_a^\circ/[\mathrm{m}])$ experimental	u_{CH_2}	immersion energy E_{head}	$\ln(K_a^\circ/[\mathrm{m}])$ calculated Eq. (38)
non-cohesive surface tension isotherms[b] sigma$_0$ = 72.2 mN/m at W|G and sigma$_0$ = 50 mN/m at W|O				
$C_nH_{2n+1}Me_2PO$ $n_C = 8\div10$, W|G [35,37]	−19.7±0.1	1.04	$-u_{CH_2}$	−20.7
$C_nH_{2n+1}Me_2N^+CH_2COO^-$ $n_C = 8\div16$, W|G [35,34][e]	−21.1±0.2	1.04		
$C_8H_{17}PEM$ $n_C = 8$, W|G [35]	−21.3±0.3	1.04		
$C_nH_{2n+1}OH$ $n_C = 8\div18$, W|O [31]	−19.0±0.2	1.39	$-u_{CH_2}$	−21.7
cohesive surface tension isotherms – gaseous region[c] sigma$_0$ = 72.2 mN/m				
C_nH_{2n+1}–OH, –Me_2PO, –SOC_2H_4OH, –Mal, –SMal, –Glu $C_{n-1}H_{2n-1}COOH$ W|G [4,35-38]	−20.7±0.3	1.04	$-u_{CH_2}$	−20.7
cohesive surface tension isotherms – LE region[d] sigma$_0$ = 50 mN/m				
$C_nH_{2n+1}OH$ $n_C = 7\div12$, W|G [35,36]	−22.1±0.3	1.39	$-u_{CH_2}$	−21.9
$C_{n-1}H_{2n-1}COOH$ $n_C = 7\div10$, W|G [35][f]	−22.2±0.2	1.39	$-u_{CH_2}$	−21.9
$C_8H_{17}SOC_2H_4OH$, W|G [38]	−22.4	1.39	$-u_{CH_2}$	−21.9
$C_{10}H_{21}SMal$, W|G [4]	−21.8	1.39	$-u_{CH_2}$	−21.9
$C_{10}H_{21}Mal$, $C_{10}H_{21}Glu$, W|G [4]	−23.0, −22.8	1.39	$-2u_{CH_2}$	−23.3
$C_nH_{2n+1}Me_2PO$ $n_C = 11\div15$, W|G [35,37]	−24.0±0.25	1.39	$-3u_{CH_2}$	−24.7
$C_nH_{2n+1}PEM$ $n_C = 9\div11$, W|G [35]	−24.9±0.2	1.39	$-3u_{CH_2}$	−24.7

[a] Cf. "List of symbols and abbreviations" for surfactants' names
[b] Data for non-cohesive surfactants, W|G or W|O interface.
[c] Data for the gaseous region of cohesive surfactants.
[d] Data for the liquid expanded (LE) region of non-cohesive surfactants.
[e] Data for pH = 7; the compound is in its zwitterionic (betaine) form.
[f] Data for undissociated acids (low pH).

Fig. 6 Experimental and theoretical intercepts of the linear dependences $\ln k_a$ vs. n_C for different homologous series

- 3. With cohesive surfactants of bulky head-groups (e.g., $C_nH_{2n+1}Me_2PO$ and $C_nH_{2n+1}PEM$), the value of $\ln K_a^\circ$ in the LE region is considerably lower than the one predicted by (38). The immersion energy for these surfactants is about $2 \div 3 \times u_{CH_2}$.
- 4. The only nonionic surfactants at W|O for which we had truly reliable data are the fatty alcohols. Their adsorption constants was found somewhat larger than the theoretical value predicted by (38) (again with one immersed C-atom): the experimental $\ln(K_a^\circ/[\mathrm{m}])$ is -19.0 vs. the theoretical value -21.7.

One way to check the reliability of the values of the transfer energy u_{CH_2} determined from the slopes of the lines in Fig. 5 is the following analysis of the experimental dependence of the surface pressure on the surfactant concentration and chain-length n_C for the two types of adsorption: cohesive and non-cohesive. Any adsorption isotherm can be written as:

$$\gamma^S(\alpha\Gamma, \beta)\Gamma = K_a C; \tag{39}$$

here γ^S is surface activity coefficient and β is attraction parameter [30]. Accounting for (37) for K_a, one obtains:

$$\gamma^S(\alpha\Gamma, \beta)\Gamma = K_a^\circ \exp(u_{CH_2} n_C / k_B T)\, C. \tag{40}$$

To simplify the analysis of the dependence $\Gamma(C; n_C)$, let us for the time being neglect the dependence of α and β on n_C. Then, one concludes from (40) that $\Gamma = \Gamma[C \times \exp(n_C u_{CH_2}/T)]$. If one substitutes this dependence into the EOS $\pi^S(\Gamma)$, one concludes that the surface pressure will depend on n_C mainly through the product $C \exp(n_C u_{CH_2}/T)$, with $u_{CH_2} = 1.04 \times k_B T$ for non-cohesive adsorption and $u_{CH_2} = 1.39 \times k_B T$ for the LE region of cohesive isotherms. This hypothesis is checked in Fig. 7 on the examples of $C_nH_{2n+1}Me_2N^+CH_2COO^-$ at W|G (non-cohesive) and $C_{n-1}H_{2n-1}COOH$ at W|G at low pH (cohesive). The data were normalized to dodecyl hydrophobic chain by subtracting 12 from n_C in the exponent, i.e., by plotting $C \exp[u_{CH_2}(n_C - 12)/T]$ on the x-axis of Fig. 7. As seen from the Figure, the results fall on a single master curve for each type of system. The slight deviations from these master-curves are due to the dependence of α and β, and π_{coh} in the case of LE, on the hydrocarbon chain length n_C, which turns out to be weaker than the main dependence on n_C in (40), as assumed above.

4.3 *Temperature Dependence of the Adsorption*

The transfer energy of a -CH_2- group from water to hydrophobic phase was extensively discussed in the classical studies on the so-called "hydrophobic effect" [21, 22]. The thermodynamic analysis of data for the temperature dependence of a large number of "hydrophobic" phenomena, such as solubility of alkanes in

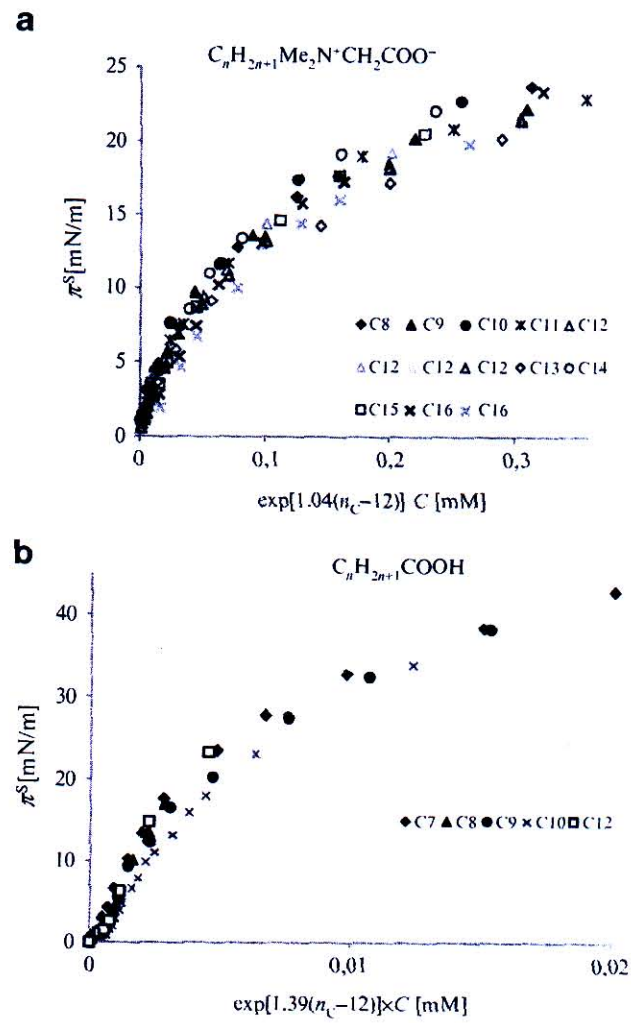

Fig. 7 Scaling of the surface tension isotherms (π^S vs. C) of homologous series of (**a**) cohesive and (**b**) non-cohesive surfactants. All data are for W|G surface. However, the data for the non-cohesive $C_nH_{2n+1}Me_2N^+CH_2COO^-$ series scales with $\exp(1.04n_C) \times C$, while the data for the LE region of $C_{n-1}H_{2n-1}COOH$ scales with $\exp(1.39n_C) \times C$, i.e., with the value $u_{CH_2}/k_BT = 1.39$ typical for W|O interface. All isotherms are reduced to a standard isotherm of the C_{12}-homologue of the respective series, see text for details. Data from [34, 35]

water, *cmc* of surfactants, etc., showed that this transfer energy is predominantly of entropic origin. It seems obvious that the nature of the free energy u_{CH_2} for *adsorption* of a methylene group in our expressions (37) and (38) is also related to the "hydrophobic" phenomena. We will use this fact to predict the temperature dependence of the adsorption constant K_a, by analyzing the tensiometric data of Vochten and Petre for the adsorption of heptanol at W|G interface [36]. The surface tension isotherms of heptanol in Fig. 8 exhibit non-zero intercepts: therefore, they are of the cohesive type. Hence, we processed the data according to the procedure outlined in Sect. 3.3 (cf. also Fig. 2a) in order to obtain the adsorption constants in the LE region at various temperatures. The results are shown in Fig. 9. We will interpret them now by using our (37) and (38) above.

The adsorption constant K_a involves large enthalpic contributions from two terms in (37) and (38), namely, the hydrophobic term $(n_C + 1)u_{CH_2}$ and the surface contribution $\alpha_\perp \sigma_0(T)/k_BT$. The hydrophobic term $(n_C + 1)u_{CH_2}$ in (37) and (38), which is the transfer free energy of the heptyl chain from water to the LE adsorption layer, must be very close to the Gibbs energy, $\Delta\mu_{0,hept}$, for transfer of a heptane

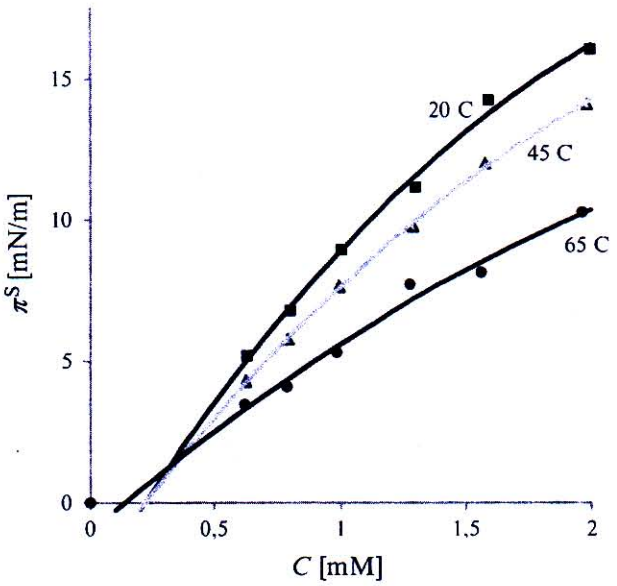

Fig. 8 Effect of the temperature on the cohesive surface pressure isotherm (π_S vs. C) of heptanol at W|G interface. Data by Vochten and Petre [36]

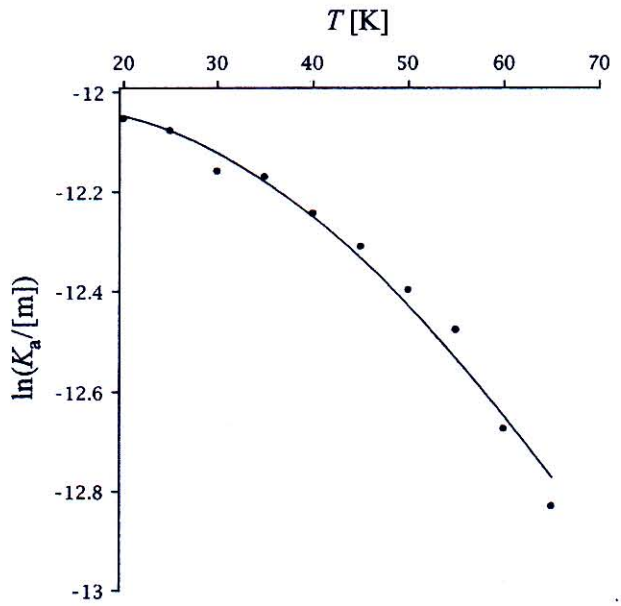

Fig. 9 Temperature dependence of the adsorption constant of heptanol at W|G in the LE region: $\ln K_a$ vs. T. The line is calculated from (43), with no adjustable parameters. Experimental points are calculated from the tensiometric data of Vochten and Petre [36]

molecule from water to heptane. The relation between these quantities must be obviously

$$\Delta\mu_{0,hept} = k_B T \ln x_s \approx -(n_C + 1)u_{CH_2}, \tag{41}$$

where x_s is the heptane molar fraction in a saturated aqueous solution. The last equation allows expressing u_{CH_2} by the measurable quantity x_s. Substituting the result in our (37) and (38) for K_a, one obtains:

$$\ln K_a = \frac{E_{head}}{k_B T} + \ln \delta_a + \frac{\alpha_\perp \sigma_0(T)}{k_B T} - \ln x_s(T). \tag{42}$$

It is convenient to normalize this equation to the standard temperature 298 K:

$$\ln K_a(T) = \ln K_a^{298} + \frac{\alpha_\perp}{k_B}\left(\frac{\sigma_0(T)}{T} - \frac{\sigma_0^{298}}{298}\right) - \ln\frac{x_s(T)}{x_s^{298}}. \tag{43}$$

Here we have neglected the weak temperature dependence of the term $\ln\delta_a + E_{head}/k_BT$ in (42). This normalization minimizes the error coming from the approximation (41). For heptanol, all quantities in the right-hand side of (43) can be easily found. The value of the constant $\ln\left(K_a^{298}/[m]\right) = -12.08$ was determined from the surface tension data at 25°C of Vochten and Petre [36]. For the LE state, the tension $\sigma_0(T)$ of the clean interface can be calculated from the equation:

$$\sigma_0 = \sigma_0^{298} - s_0(T - 298), \tag{44}$$

which is based on tensiometric data for water|alkane interface [39]. Here $s_0 = 0.09\,\mathrm{mJ/Km^2}$ is entropy and $\sigma_0^{298} = 50\,\mathrm{mJ/m^2}$ is the interfacial tension of W|alkane at 25°C [39]. The molecular area is $\alpha_\perp = 16.5\,\mathrm{Å}^2$. Finally, from [40], the temperature dependence of $\ln x_s$ in the range 20°C÷70°C is:

$$\ln x_s = \ln x_s^{298} + \frac{\Delta h_s^{298} - 298\Delta c_{p,s}}{R}\left(\frac{1}{T} - \frac{1}{298}\right) - \frac{\Delta c_{p,s}}{R}\ln\frac{T}{298}, \tag{45}$$

where x_s^{298} is the solubility at 298 K ($\ln x_s^{298} = -14.61$), $\Delta h_s^{298} = 2149\,\mathrm{J/mol}$ is the molar enthalpy of dissolution at 298 K, $\Delta c_{p,s} = -473.6\,\mathrm{J/molK}$ is the heat capacity of dissolution [40], R is gas constant. Substituting (44) and (45) in (43) yields an explicit expression for $\ln K_a(T)$. The results for $\ln K_a(T)$ calculated in this way from (43) are shown by continuous curve in Fig. 9 and compared with experimental results. The agreement is good.

From (43), the enthalpy of adsorption Δh_a can be calculated according to Gibbs–Helmholtz relation:

$$\Delta h_a = -k_BT^2\frac{\partial \ln K_a}{\partial T} = \alpha_\perp h_0 - \Delta h_s/N_A, \tag{46}$$

where $h_0 = \sigma_0 + Ts$ is the enthalpy per unit area of the W|O interface and $\Delta h_s = \Delta h_s^{298} + (T-298)\Delta c_{p,s}$ is the molar enthalpy of dissolution of heptane. The second "hydrophobic" term on the right hand side of (46), $\Delta h_s/N_A$, is a linear function of T; it is zero at 30°C, and reaches $6 \div 7 \times k_BT$ at 70°C. The first "surface" term, $\alpha_\perp h_0 = 1.3\times10^{-20}\,\mathrm{J}$, is about $3\times k_BT$. Therefore, the surface term is by no means negligible. On the contrary, it is the leading effect at room temperature.

The cohesive pressure π_{coh} of heptanol also varies with T. It can be shown that, starting from 3.0 mN/m at 20°C, it decreases with slope 0.044 mN/m × K. One can then expect that π_{coh} will become zero at 90°C and the LE state will cease to exist, and the adsorption layer will become non-cohesive. This effect is similar to the effect of the decrease of the number of -CH_2- groups on π_{coh} in Fig. 4.

5 Conclusions

Our analysis of the experimental data for the surface and interfacial tension of more than 50 nonionic surfactants revealed that the data can be described by one of two characteristic isotherms: of cohesive and non-cohesive type. Three phenomenological criteria were formulated for relating given set of tensiometric data to one of these types.

The most important ***first criterion*** is the existence of a kink in the cohesive isotherms at low concentration (cf. Fig. 2a). The low-concentration region before the kink corresponds to gaseous state of the adsorption layer [4]. The $\pi^S(C)$-dependence after the kink exhibits negative intercept $-\pi_{coh}$ (Fig. 2a). This intercept $-\pi_{coh}$ is in fact Langmuir's *cohesive (spreading) pressure* [2, 10]. The kink itself probably corresponds to a first order phase transition [4, 5]. If no kink is present, the surface tension isotherm is non-cohesive.

Unfortunately, it is often problematic to obtain reliable measurements in the gaseous region of a cohesive isotherm, and consequently it is not always easy to observe the kink. If such is the case, a ***second criterion*** can be used: all surfactants which form non-cohesive monolayers follow (at least qualitatively) the HFL isotherm, with area parameter equal or very close to the actual area of the surfactant tail ($\alpha = 16.5\,\AA^2$ for surfactants with linear hydrocarbon tail and small polar head-group), cf. Fig. 2. In contrast, the data for cohesive films cannot be interpolated satisfactory with HFL model.

The ***third criterion*** is related to the linear dependence of the logarithm of adsorption constant $\ln K_a$ on the number n_C of carbon atoms of the surfactant, cf. (Fig. 5a). The slope of this dependence for non-cohesive type of isotherms is $\mathrm{d}\ln K_a/\mathrm{d}n_C = 1.04$. For the LE region of *cohesive* isotherms at W|G, the slope is 1.39 (Fig. 5c)—a value typical, in fact, for the W|O interface. The different slopes are related to the different transfer energies u_{CH_2} of a methylene group from water to gas and from water to LE adsorption layer. The latter is in fact a transfer to an oil-like environment.

The adsorption at W|O interface always exhibits non-cohesive behavior. Cohesive isotherms are typical for W|G only. However, not always the adsorption at W|G is cohesive (cf. Fig. 6), e.g., the isotherms of $C_nH_{2n+1}Me_2N^+CH_2COO^-$ at W|G exhibit no LE region (Fig. 7a). We have also found that within certain homologous series of surfactants, both types can be found: short-chain homologues are non-cohesive, while long-chained ones are cohesive (a typical example is $C_nH_{2n+1}Me_2PO$, cf. Fig. 5). The chain-length at which the transition from cohesive to non-cohesive behavior occurs corresponds to zero cohesive pressure (Fig. 4).

We further compared in Fig. 6 the experimentally determined adsorption constants to the model, previously developed by us (presented in Sect. 2). The model does not involve adjustable parameters. In most cases, the comparison is satisfactory, if one assumes that one C-atom from the hydrocarbon chain remains immersed into water (Fig. 6). We further checked our model by comparing its predictions to experimental data for the temperature T dependence of the adsorption constant

(Fig. 9). Independent data for the dependence on T of the transfer energy of the hydrocarbon chain from water to oil phase were used to model the transfer from water to liquid expanded monolayer at W|G. The agreement reached without using adjustable parameters is very good. This proves beyond doubt both Langmuir's concept for the LE state, and our model of the adsorption constant.

We also observed couple of effects which are waiting for explanation. The first one is the dependence of the cohesive pressure on the surfactant's chain-length and head-group (Fig. 4). An important open question is the equation of state of dense LE monolayer of nonionic surfactants. The comparison between results presented here for the nonionic surfactants and those obtained previously in [6] for ionic surfactants is also forthcoming.

Acknowledgement This work was supported by Bulgarian National Science Fund Grants DDVU 02/12 and DDVU 02/54.

References

1. Adam, N.K.: Proc. Roy. Soc. A **101**, 516 (1922)
2. Langmuir, I.: J. Chem. Phys. **1**, 756–776 (1933)
3. Adam, N.K.: The Physics and Chemistry of Surfaces. Clarendon, Oxford (1941)
4. Kumpulainen, A.J., Persson, C.M., Eriksson, J.C., Tyrode, E.C., Johnson, C.M.: Langmuir **21**, 305–315 (2005)
5. Mufazzal Hossain, Md., Suzuki, T., Iimura, K., Kato, T.: Langmuir **22**, 1074–1078 (2006)
6. Slavchov, R.I., Karakashev, S.I., Ivanov, I.B.: Ionic surfactants and ion-specific effects: adsorption, micellization, thin liquid films, Chapter 2. In: Römsted L. (ed.)Surfactant Science and Technology: Retrospects and Prospects. Taylor and Francis, LLC, Boca Raton (2013)
7. Aratono, M., Uryu, S., Hayami, Y., Motomura, K., Matuura, R.: J. Colloid Interface Sci. **98**, 33–38 (1984)
8. Kaganer, V.M., Möhwald, H., Dutta, P.: Rev. Mod. Phys. **71**, 779–819 (1999)
9. Davies, J.T.: J. Colloid Sci. **11**, 377–390 (1956)
10. Davies, J.T., Rideal, E.: Interfacial Phenomena. Academic, New York (1963)
11. Smith, T.: J. Colloid Interface Sci. **23**, 27–35 (1967)
12. Möhwald, H.: Rep. Rog. Phys. **56**, 653–685 (1993)
13. Fischer, T.M., Lösche, M.: Lect. Notes Phys. **634**, 383 (2004)
14. Shchukin, E.D., Pertsov, A.V., Amelina, E.A.: Colloid Chemistry. University Press, Moscow (1982) [in Russian]. Elsevier, Amsterdam (2001) [in English]
15. Kralchevsky, P.A., Danov, K.D., Broze, G., Mehreteab, A.: Langmuir **15**, 2351–2365 (1999)
16. Danov, K.D., Kralchevsky, P.A., Ananthapadmanabhan, K.P., Lips, A.: J. Colloid Interface Sci. **300**, 809–813 (2006)
17. Ivanov, I.B., Ananthapadmanabhan, K.P., Lips, A.: Adv. Colloid Interface Sci. **123–126**, 189–212 (2006)
18. Lange, H., Jeschke, P.: Surface monolayers, Chapter 1, pp. 1–44. In: Schick, M.J. (ed.) Nonionic Surfactants. Physical Chemistry. Surfactant Science Series, vol. 21. Marcel Dekker, New York (1987)
19. Hückel, W.: Theoretical Principles of Organic Chemistry, vol. II, p. 435. Elsevier, New York (1958)
20. Kitaigorodskii, A.I.: Organic Chemical Crystallography. Consultant Bureau, New York (1961)
21. Tanford, C.: The Hydrophobic Effect. Wiley, New York (1980)

22. Israelachvili, J.N.: Intermolecular and Surface Forces. Academic, New York (2011)
23. Hill, T.L.: An Introduction to Statistical Thermodynamics. Addison-Wesley, Reading (1962)
24. Davies, J.H.: The Physics of Low-Dimensional Semiconductors - An Introduction. Cambridge University Press, Cambridge (1998)
25. Levich, V.G.: Introduction to Statistical Physics. Gos. Izd. Tekhn.-Teor. Lit., Moscow (1954)
26. Langmuir, I.: J. Am. Chem. Soc. **40**, 1361–1403 (1918)
27. Volmer, M.: Z. Phys. Chem. **115**, 253–260 (1925)
28. Tonks, L.: Phys. Rev. **50**, 955–963 (1936)
29. Helfand, E., Frisch, H.L., Lebowitz, J.L.: J. Chem. Phys. **34**, 1037–1042 (1961)
30. Ivanov, I.B., Danov, K.D., Dimitrova, D., Boyanov, M., Ananthapadnamabhan, K.P., Lips, A.: Colloids Surf. A **354**, 118–133 (2010)
31. Aveyard, R., Briscoe, B.J.: J. Chem. Soc. Faraday Trans. I **68**, 478–491 (1972)
32. Aveyard, R., Briscoe, B.J., Chapman, J.: J. Chem. Soc. Faraday Trans. I **69**, 1772–1778 (1973)
33. Villalonga, F.A., Koftan, R.J., O'Connell, J.P.: J. Colloid Interface Sci. **90**, 539 (1982)
34. Wüstneck, R., Miller, R., Kriwanek, J., Holzbauer, H.-R.: Langmuir **10**, 3738 (1994)
35. Fainerman, V.B., Miller, R., Aksenenko, E.V., Makievski, A.V.: Equilibrium adsorption properties of single and mixed surfactant solutions, Chapter 3, pp. 189–286. In: Fainerman, V.B., MRobius, D., Miller, R. (eds.) Surfactants – Chemistry, Interfacial Properties, Applications
36. Vochten, R., Petre, G.: J. Colloid Interface Sci. **42**, 320–327 (1973)
37. Warszynski, P., Lunkenheimer, K.: J. Phys. Chem. B **103**, 4404–4411 (1999)
38. Aratono, M., Uryu, S., Hayami, Y., Motomura, K., Matuura, R.: J. Colloid Interface Sci. **98**, 33–38 (1984)
39. Goebel, A., Lunkenheimer, K.: Langmuir **13**, 369–372 (1997)
40. Tsonopoulos, C.: Fluid Phase Equilib. **156**, 21–33 (1999)